Interaction of H_2S with the X/MoS_2 Surface (X = Zn, Cu, Ni, Co). A Theoretical Study

Anibal Sierraalta,* Armando Herize, and Rafael Añez

Laboratorio de Química Computacional, Centro de Química, Instituto Venezolano de Investigaciones Científicas, Apartado 21827, Caracas 1020-A, Venezuela

Received: January 17, 2001; In Final Form: April 9, 2001

Calculations for H_2S adsorption on X/MoS_2 catalysts modeled by $XMo_2S_{10}H_6$ (X = Zn, Cu, Ni, Co) clusters were carried out using ab initio Hartree−Fock and pseudopotential approaches. Two vertical adsorption modes were studied. The analysis of the electronic properties show that the adsorption energy depends not only on the metal promoter (Zn, Cu, Ni, or Co) but also on the electronic state of the $Mo_2S_{10}H_6$ moiety, which determine the electron distribution of the X atom. Results obtained optimizing the adsorbate geometry on the metallic center indicate that a small charge transfer from the H_2S molecule to the $XMo_2S_{10}H_6$ cluster occurs and the interaction phenomenon corresponds to a physisorption.

Introduction

Hydrodesulfurization (HDS) or the removal of the sulfur-containing molecules is a crucial step in the refinement process of heavy oil. The HDS reaction, at the industrial level, is performed over heterogeneous catalysts using promoted molybdenum disulfide (MoS_2) anchored over a nonreactive support, such as γ-alumina.[1−2] In general, these catalysts are mixtures of MoS_2 with Co or Ni. It is well-known that both metals (Co and Ni) have strong promoter effect while the remaining first row transition metals only have a moderate or weak effect on the catalysis of HDS.[3−4]

Experimental[1,5−8] and theoretical[4,8−14] works have been done on first row transition metal-promoted MoS_2 catalysts. Various models for the structure of the active site of the catalyst have been proposed in the literature.[1] Startsev[1] has suggested the "sulfide bimetallic species" model (SBMS) in order to explain the reactivity of the bimetallic sulfide catalysts (*Metal*−MoS_2; *Metal* ≠ Mo) in HDS reactions. According to this model, the important step in the catalytic reaction is the adsorption of the sulfide species on the *Metal*, followed by a hydrogenation step. Zakarov et al.,[10] in a quantum chemical study performed on a Ni−$Mo_2S_{10}H_{10}$ molecular aggregate, proposed that both, the initial and final step of the catalytic cycle is the adsorption of the H_2S molecule on the *Metal*. From the analysis of Ni oxidation states and the adsorption energies the authors concluded that the active site of the bimetallic species or the active component of the HDS catalyst, a Ni(IV) with a d^6 electronic configuration, is stabilized by the H_2S adsorption.[10,11] In a recent work on Co/MoS2 catalyst, Zakharov and Startsev[12] propound that after H_2S adsorption on the Co atom the d^6 electronic configuration of the Co is stabilized.

The interaction of the H_2S with the catalytic surface is complex. For instance, literature shows that the H_2S inhibits the HDS reactions.[15−17] Isotopic exchange studies show that the sulfur atom of the H_2S molecule can be exchanged with the sulfur surface atoms of the catalyst.[17−21] On the other hand, there are indications that the H_2S adsorption on the active center favors the d^6 state of the Ni and Co atoms in the NiMoS and CoMoS catalysts.[22] Some studies point out that the release of H_2S from labile sulfur may be the rate-determining step in the catalytic cycle.[17,21]

Details of the manner in which H_2S binds to the surface of the metal sulfides are unknown. Adsorption studies as well as interaction energies and charge transfer studies are of particular interest for the understanding of this phenomenon. A fairly large number of publications on this topic show that considerable effort has been devoted to this problem. Despite this, there is still need for more experimental and theoretical studies to fully understand the H_2S interaction with the catalytic surface.

The present work was undertaken in order to understand the interaction of H_2S with *Metal*−MoS_2 surfaces. It presents the analysis of the electronic interaction of the H_2S molecule with different cluster models (X−MoS_2, X = Co, Ni, Cu, Zn), using ab initio self-consistent-field (SCF) calculations and the SBMS model proposed by Startsev.[1]

Computational Details

All calculations and geometry optimizations were performed using the Gaussian-94 program[23] at HF−SCF level. The basis sets and the relativistic compact effective potentials, that include explicitly the $(n-1)s^2$, $(n-1)p$,[6] $(n-1)d^x$ and $(n)s^y$ electrons from Stevens et al.[24] were used for Co, Ni, Cu, Zn atoms. The LANL1DZ effective core potential with its valence shell basis set, both provided by the Gaussian-94 package, were employed for all S cluster atoms. All H atoms were described using the 6-31G** basis set. The H_2S molecule was described with all their electrons, using the 6-31G basis set for S atom taking from the Gaussian-94 library. According to the literature,[8] these basis sets provide good results for adsorption geometries. The large core of Wadt and Hay ECP, that include only the $(n-1)d^x$ and $(n)s^y$ electrons, was employed for Mo atom with the following contraction scheme (3s3p4d/2s1p2d). The electronic charge distribution of the clusters was analyzed using the natural bond orbital (NBO) partition scheme.[25−26] All the calculations were performed on the neutral systems. Charged systems were not considered. To test the quality of the basis sets employed in this work, calculations for the dissociation energies of the CoS, NiS, CuS, and ZnS diatomic molecules were performed. The calculations predict correctly the experimental[27] trend of the bonding energies, i.e, NiS(4.0 ev) > CoS(3.3 ev) > CuS-(1.8 ev) > ZnS(1.7 ev).

* Corresponding author.

10.1021/jp010195c CCC: $20.00
Published on Web 06/12/2001

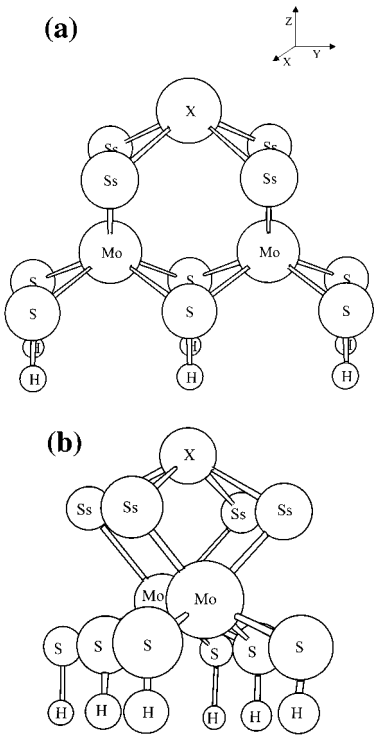

Figure 1. Schematic representation of the $XMo_2S_{10}H_6$ cluster. (a) Front view. (b) Lateral view.

Calculations of molecular aggregates with more than one metallic atom are difficult due to the presence of a large amount of electronic states. It is well-known that the spin multiplicity is one of the variables that characterize the states. Therefore, it is necessary to search into all possible spin multiplicities in order to find the ground-state. Taking into account this problem we performed for each spin multiplicity, calculations with geometry optimization using the first twenty single excitations from the HF-determinant of the corresponding spin state.

Cluster Models

Four different systems $XMo_2S_{10}H_6$ (X = Zn, Cu, Ni, Co) were studied in order to analyze the electronic properties of the SBMS model. All $Mo_2S_{10}H_6$ clusters have four layers, the first and the third contain S atoms, the second layer Mo atoms, and the last one only H atoms. The hydrogen atoms were used to avoid the problem of "orbitals that point to anywhere".[28,29] The metal atom X was set directly on the sulfur basal plane of MoS_2, according to the SBMS model and the experimental results of Topsoe[30] and Bouwens[31] (See Figure 1). In all calculations the X−S or X−Mo and S−H bond distances were optimized. The Mo−S and S−S distances of the $Mo_2S_{10}H_6$ were kept constant and set equal to those reported for bulk MoS_2.[32] The clusters models used in this work are similar to others currently used in the literature.[10−12,33−34]

For the adsorption study of H_2S on $XMo_2S_{10}H_6$, two vertical adsorption modes were considered (Mode A and Mode B). For mode A, the H_2S molecule was set in the *YZ* plane (see Figure 2a). For mode B, the H_2S molecule was set in the *XZ* plane (see Figure 2b). In all calculations the X−Mo, H_2S−X, H−S (in H_2S)−and S−H (in $XMo_2S_{10}H_6$) bond distances were optimized as well as the HSH angle of the H_2S molecule.

Results and Discussion

Vertical Adsorption. Mode A. The geometrical and electronic properties for the first five lowest energy states of the

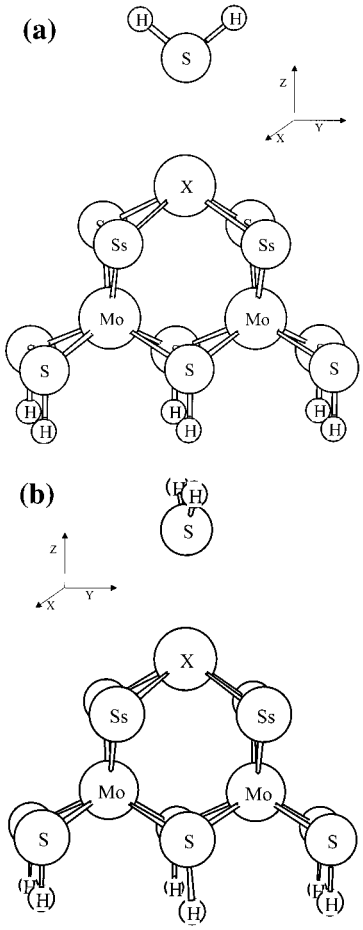

Figure 2. Molecular geometry of the H_2S sorbed on $XMo_2S_{10}H_6$ cluster (X = Co, Ni, Cu, Zn). (a) Mode A. (b) Mode B.

TABLE 1: Geometrical and Electronic Properties of $ZnMo_2S_{10}H_6$ Cluster

electronic state	Zn−Ss (Å)	SD(Ss)	Q_{Mo}	Q_{Ss}	Q_{Zn}	4sp[a]	ΔE[b] (kcal/mol)
$^{11}B_2$	2.42	0.93	−0.08	−0.37	+1.46	0.54	0.00
$^{9}A_1$	2.43	0.64	−0.06	−0.45	+1.48	0.52	+7.78
$^{13}A_2$	2.43	1.09	+0.04	−0.32	+1.42	0.58	+10.03
$^{11}A_2$	2.42	0.90	−0.10	−0.37	+1.43	0.57	+18.87
$^{13}B_2$	2.43	0.87	+0.02	−0.49	+1.48	0.52	+21.60

[a] Electronic population of the Zn 4sp orbitals. For all states, 3d electron population: $3d_{xy}(2.00)$, $3d_{xz}(2.00)$, $3d_{yz}(2.00)$, $3d_{x^2-y^2}(2.00)$, and $3d_{z^2}(2.00)$. [b] Energy difference between the corresponding electronic state and the $^{11}B_2$ state.

$ZnMo_2S_{10}H_6$ cluster are listed in Table 1. The analysis of these results shows that (a) the lowest energy state for the $ZnMo_2S_{10}H_6$ corresponds to an $^{11}B_2$ state; (b) the distance of Zn to the sulfur surface atoms (Zn−Ss) does not change with the electronic state even though there is 21.6 kcal/mol between the $^{11}B_2$ and the $^{13}B_2$ states; (c) the variation in the spin multiplicity corresponds roughly to the variation of the spin density of the sulfur surface atoms (SD (Ss)); (d) the atomic charge of the Mo (Q_{Mo}), Ss (Q_{Ss}), and Zn (Q_{Zn}) atoms changes with the electronic state of the aggregate; and (e) the positive charge on the Zn atom is due to the partial loss of the 4s electrons.

The analysis of the data allows us to conclude that the energy difference between the electronic states ($^{11}B_2$, $^{9}A_1$, $13A_2$, $11A_2$, and $13B_2$) is associated mainly, with the electronic distribution of the $Mo_2S_{10}H_6$. For example, the $^{13}B_2$ state is 13.82 kcal/mol higher in energy than the $^{9}A_1$ state but the electronic distribution of the Zn atom is the same for both states as well as the Zn−Ss

TABLE 2: Calculated Properties of H_2S Adsorption on $ZnMo_2S_{10}H_6$ Cluster

Geometrical Properties

electronic state	Zn−Ss (Å)	H_2S−Zn (Å)	H−S[a] (Å)	HSH[a] (deg)	ΔE[b] (kcal/mol)	[c]E_{ads} (kcal/mol)
$^{11}B_2$	2.46	2.67	1.33	100.8	0.00	7.62
$^{9}A_1$	2.47	2.63	1.33	101.2	+6.81	8.59
$^{13}A_2$	2.47	2.61	1.33	101.5	+7.70	9.95
$^{11}A_2$	2.46	2.64	1.33	101.2	+17.86	8.63
$^{13}B_2$	2.46	2.67	1.33	100.7	+22.10	7.12

Electronic Properties

electronic state	SD(Ss)	Q_{Mo}	Q_{Ss}	Q_{Zn}	4sp[d]	Q_{H_2S}
$^{11}B_2$	0.93	−0.06	−0.39	+1.47	0.53	+0.05
$^{9}A_1$	0.65	−0.05	−0.46	+1.48	0.52	+0.06
$^{13}A_2$	1.09	+0.05	−0.34	+1.43	0.58	+0.06
$^{11}A_2$	0.90	−0.08	−0.38	+1.44	0.57	+0.06
$^{13}B_2$	0.87	+0.03	−0.50	+1.48	0.52	+0.05

[a] Geometry for the free H_2S molecule: H−S = 1.33 Å, HSH = 95.7°. [b] Energy difference between the corresponding electronic state and the $^{11}B_2$ state. [c] Adsorption energy. [d] Electronic population of the Zn 4sp orbitals. For all states, 3d electron population: $3d_{xy}(2.00)$, $3d_{xz}(2.00)$, $3d_{yz}(2.00)$, $3d_{x^2-y^2}(2.00)$, and $3d_{z^2}(2.00)$.

distance. On the other hand, the net charges and the spin density of the atoms that belong to the $Mo_2S_{10}H_6$ moiety are different (+0.02 and −0.06 for Q_{Mo}, −0.49 and −0.45 for Q_{Ss}, 0.87 and 0.64 for SD(Ss)), showing that the $^{13}B_2$ and $^{9}A_1$ states are characterized by the electronic properties of the $Mo_2S_{10}H_6$ and not for the electronic state of the Zn atom.

Table 2 reports the electronic properties of the H_2S−$ZnMo_2S_{10}H_6$ system. For all states a charge transfer (Q_{H_2S}) around 0.06e from the H_2S molecule to the $ZnMo_2S_{10}H_6$ cluster occurs. This charge is received by the $Mo_2S_{10}H_6$ moiety and not by the Zn atom. It shows that the $Mo_2S_{10}H_6$ structure contribute to the stabilization of the H_2S−$ZnMo_2S_{10}H_6$ system by receiving the transferred charge from the adsorbed molecule.

The calculated adsorption energies (E_{ads}) show a range of values between 7.12 and 9.95 kcal/mol. The order in the E_{ads} follow, approximately, the inverse order of the H_2S−Zn distance, i.e., the highest value of adsorption energy (9.95 kcal/mol) is associated with the smallest H_2S−Zn distance (2.61 Å) and vice versa the lowest energy value (7.12 kcal/mol) with the largest distance (2.67 Å). Even though the electronic distribution of the Zn atom is the same for the $^{13}B_2$ and $^{9}A_1$ states in the H_2S−$ZnMo_2S_{10}H_6$ and in the $ZnMo_2S_{10}H_6$ clusters (see Tables 2 and 1), the calculated adsorption energies are different (7.62 and 8.07 kcal/mol for $^{13}B_2$ and $^{9}A_1$ states, respectively). This difference in adsorption energies may be due to the theoretical level used. It is well-known[8,35] that at HF level the computed binding energies are not quantitative and only provide a guide for the interpretation of experimental results. Beside this, an incomplete cancellation of the electronic effect of the $Mo_2S_{10}H_6$ moiety must occur. Therefore the adsorption energies calculated as the difference between the total energy of H_2S−$ZnMo_2S_{10}H_6$ and the total energy of $ZnMo_2S_{10}H_6$ plus the H_2S free, are not equals. The magnitudes of the E_{ads} and Q_{H_2S} values as well as the changes in the H−S distance and H−S−H angle of the H_2S molecule show that the sorption of H_2S on $ZnMo_2S_{10}H_6$ corresponds to a physisorption instead of a chemisorption.

TABLE 4: Calculated Properties of H_2S Adsorption on $CuMo_2S_{10}H_6$ Cluster

Geometrical Properties

electronic state	Cu−Ss (Å)	H_2S−Cu (Å)	H−S (Å)	HSH (deg)	ΔE[a] (kcal/mol)	E_{ads} (kcal/mol)
$^{12}B_1$	2.40	2.86	1.33	99.1	0.000	4.57
$^{10}A_2$	2.41	2.79	1.33	99.5	+8.35	5.34
$^{10}A_2$	2.41	2.78	1.33	99.8	+9.70	5.68
$^{12}A_1$	2.41	2.71	1.33	100.3	+15.12	8.10
$^{10}A_1$	2.42	2.76	1.33	99.9	+18.47	6.51

Electronic Properties

electronic state	Q_{Mo}	Q_{Ss}	Q_{Cu}	Q_{H_2S}	SD(Ss)	SD(Cu)	4sp[b]	$3d_{xy}$[c]
$^{12}B_1$	−0.06	−0.36	+1.39	+0.03	0.96	0.90	0.46	1.12
$^{10}A_2$	−0.06	−0.43	+1.41	+0.04	0.68	0.90	0.40	1.11
$^{10}A_2$	−0.11	−0.38	+1.40	+0.04	0.82	0.90	0.40	1.12
$^{12}A_1$	+0.05	−0.28	+1.35	+0.05	1.07	0.90	0.43	1.13
$^{10}A_1$	+0.05	−0.39	+1.39	+0.04	0.85	0.90	0.40	1.12

[a] Energy difference between the corresponding electronic state and the $^{12}B_1$ state. [b] Electronic population of the Cu 4sp orbitals. [c] 3d electron population was: $3d_{xz}(2.00)$, $3d_{yz}(2.00)$, $3d_{x^2-y^2}(2.00)$, and $3d_{z^2}(2.00)$.

Table 3 shows the geometrical and electronic properties of the $CuMo_2S_{10}H_6$ cluster. The distance of Cu to the sulfur surface atoms (Cu−Ss) does not change with the $CuMo_2S_{10}H_6$ electronic states and for all states, the Cu atom has one unpaired electron localized in the $3d_{xy}$ orbital. This orbital is in the plane of the four sulfur surface atoms and therefore it is not expected to interact with the H_2S molecule. The atomic charge of Mo (Q_{Mo}), Ss (Q_{Ss}), Cu (Q_{Cu}) and the SD(Ss) change with each electronic state of the aggregate. As in the case of the Zn atom, the positive charge of Cu atom comes from a charge transfer from the Cu atom to the $Mo_2S_{10}H_6$ moiety.

The geometrical and electronic properties for the H_2S adsorption on the $CuMo_2S_{10}H_6$ cluster are reported in Table 4. Several features can be obtained from the analysis of these data: (a) the distance between the Cu and the sulfur surface atoms (Cu−Ss) is independent of the electronic state of H_2S−$CuMo_2S_{10}H_6$ cluster; (b) the H−S distance does not change and only small variations in the HSH angle were obtained; (c) the H_2S−Cu distance shows a larger spread than in the case of H_2S−Zn; (d) two $^{10}A_2$ electronic states were found that, according to Table 4, are characterized by the electronic population of the atoms that belong to the $Mo_2S_{10}H_6$ (−0.06 and −0.11 for Q_{Mo}, −0.43 and −0.38 for Q_{Ss}, 0.68 and 0.82 for SD(Ss), respectively); (e) after the adsorption the Cu atom keeps the unpaired electron (SD(Cu) = 0.90) in the $3d_{xy}$ orbital[1] ([1]for the pseudopotential used in this work the Cu ground-state configuration corresponds to $3d^9 4s^2$). Due to the orbital geom-

TABLE 3: Geometrical and Electronic Properties of $CuMo_2S_{10}H_6$ Cluster

electronic state	Cu−S(Å)	SD(Ss)	Q_{Mo}	Q_{Ss}	Q_{Cu}	4sp[a]	$3d_{xy}$[b]	SD(Cu)	ΔE[c] (kcal/mol)
$^{12}B_1$	2.37	0.97	−0.08	−0.35	+1.35	0.49	1.14	0.89	0.000
$^{10}A_2$	2.38	0.68	−0.07	−0.42	+1.39	0.46	1.13	0.89	+9.12
$^{10}A_2$	2.38	0.84	−0.12	−0.37	+1.38	0.47	1.14	0.88	+10.81
$^{12}A_1$	2.38	1.08	+0.03	−0.27	+1.32	0.50	1.15	0.88	+18.65
$^{10}A_1$	2.39	0.85	+0.03	−0.36	+1.37	0.47	1.14	0.88	+20.41

[a] Electronic population of the Cu 4sp orbitals. [b] 3d electron population: $3d_{xz}(2.00)$, $3d_{yz}(2.00)$, $3d_{x^2-y^2}(2.00)$, and $3d_{z^2}(2.00)$. [c] Energy difference between the corresponding electronic state and the $^{12}B_1$ state.

TABLE 5: Geometrical and Electronic Properties of $NiMo_2S_{10}H_6$ Cluster

electronic state	Ni−Ss (Å)	SD(Ss)	Q_{Mo}	Q_{Ss}	Q_{Ni}	4sp[a]
$^{15}B_2$	2.41	1.08	+0.10	−0.33	+1.37	0.47
$^{13}B_1$	2.40	0.98	−0.09	−0.35	+1.39	0.45
$^{13}A_1$	2.41	0.96	−0.07	−0.36	+1.39	0.47
$^{11}A_2$	2.42	0.67	−0.07	−0.44	+1.45	0.43
$^{15}A_1$	2.42	0.90	+0.02	−0.47	+1.41	0.45

electronic state	$3d_{xy}$	$3d_{xz}$	$3d_{yz}$	$3_{dx^2-y^2}$	$3d_{z^2}$	SD(Ni)	ΔE[b] (kcal/mol)
$^{15}B_2$	1.12	1.02	2.00	2.00	1.99	1.89	0.000
$^{13}B_1$	1.11	2.00	2.00	2.00	1.03	1.89	+3.78
$^{13}A_1$	1.11	1.02	2.00	2.00	1.99	1.89	+11.72
$^{11}A_2$	1.09	2.00	2.00	2.00	1.01	1.91	+15.09
$^{15}A_1$	1.11	1.02	2.00	2.00	1.99	1.89	+33.29

[a] Electronic population of the Ni 4sp orbitals. [b] Energy difference between the corresponding electronic state and the $^{15}B_2$ state.

etry, the $3d_{xy}$ electrons do not have a strong interaction with the H_2S lone pair, which is in the *XZ* plane. Therefore, the H_2S interaction is done across the 4sp orbitals of the Cu atom. Even though for all the electronic states, the electron distribution of the Cu atom is almost the same, the E_{ads} values show a range from 4.57 kcal/mol to 8.10 kcal/mol.

In the case of the cluster with Ni atom, a more complex situation is present, the electronic states of the $NiMo_2S_{10}H_6$ are characterized for the electronic distribution of the $Mo_2S_{10}H_6$ moiety and for the 3d occupancies of the Ni atom (See Table 5). For example in the $^{15}B_2$, $^{13}A_1$ and $^{15}A_1$ electronic states, the Ni atom has the same electronic distribution but the net charge distribution of the Mo and S surface atoms is different. For the $^{13}B_1$ and $^{11}A_2$ states, beside the proper charge distribution of the $Mo_2S_{10}H_6$ moiety, there is a different distribution of the 3d electrons of the Ni atom. In the $^{13}B_1$ and $^{11}A_2$ states the unpaired electrons are localized in the $3d_{xy}$ and 3_{dz^2} orbital, while for the $^{15}B_2$, $^{13}A_1$, and $^{15}A_1$ states these electrons occupied the $3d_{xy}$ and $3d_{xz}$ orbital. As in the previous cases of Zn and Cu clusters, the positive charge on Ni atom is due to the partial transfer of the 4s electrons to the $Mo_2S_{10}H_6$ moiety. The variation in the spin multiplicity of the states corresponds, approximately, to the variation of the SD of the sulfur surface atoms. Experiments on NiMoS catalyst, using EXASF and XANES spectroscopies,[30,31] have shown that the most probable geometry for Ni atom is a tetragonal pyramidal structure with a Ni−Ss distance of 2.21−2.24 Å and one sulfur atom at 2.11 Å. The theoretical value obtained herein (2.41 Å) is in agreement with the experimental one, considering the theoretical level (HF) and the fact that in the cluster model used the Ni atom is only bonded to four S atoms.

The geometrical and electronic properties of H_2S adsorption on the $NiMo_2S_{10}H_6$ cluster are reported in Table 6. In general, the Ni−Ss and S−H distances do not change with the electronic state and only variations in the H_2S−Ni distance and HSH angle are observed. The E_{ads} values show a range of values between 5.55 and 9.27 kcal/mol, the adsorption energy being equal to 8.74 kcal/mol for the lowest energy electronic state. Zakharov and co-workers[10] studied the adsorption of H_2S on $NiMo_2S_{10}H_{10}$ at MP2 level for the $^1A_1$ state. They found for the lowest energy state, a value of 2.77 Å for the H_2S−Ni distance and 8.62 kcal/mol for the adsorption energy. These values are similar to ours (2.71 Å and 8.74 kcal/mol). Unfortunately, they did not analyze the problems of the spin multiplicity and the cancellation of the support in the calculations of the adsorption energies. For

TABLE 6: Calculated Properties of H_2S Adsorption on $NiMo_2S_{10}H_6$ Cluster

Geometrical Properties

electronic state	Ni−Ss (Å)	H_2S−Ni (Å)	H−S (Å)	HSH (deg)	ΔE[a] (kcal/mol)	E_{ads} (kcal/mol)
$^{15}B_2$	2.45	2.71	1.33	100.4	0.000	8.74
$^{13}B_1$	2.43	2.67	1.33	100.8	+4.45	8.07
$^{13}A_1$	2.44	2.81	1.33	99.7	+14.34	6.12
$^{11}A_2$	2.46	2.63	1.33	101.2	+14.56	9.27
$^{15}A_1$	2.45	2.81	1.33	99.6	+36.48	5.55

Electronic Properties

electronic state	Q_{Mo}	Q_{Ss}	Q_{Ni}	Q_{H_2S}	SD(Ss)	SD(Ni)
$^{15}B_2$	+0.11	−0.35	+1.38	+0.05	1.08	1.90
$^{13}B_1$	−0.07	−0.36	+1.40	+0.05	0.97	1.88
$^{13}A_1$	−0.05	−0.37	+1.41	+0.04	0.96	1.90
$^{11}A_2$	−0.05	−0.44	+1.44	+0.06	0.67	1.91
$^{15}A_1$	+0.04	−0.48	+1.43	+0.03	0.90	1.90

electronic state	4sp[b]	$3d_{xy}$	$3d_{xz}$	$3d_{yz}$	$3d_{x^2-y^2}$	$3d_{z^2}$
$^{15}B_2$	0.47	1.10	1.03	2.00	2.00	1.99
$^{13}B_1$	0.45	1.09	2.00	2.00	2.00	1.04
$^{13}A_1$	0.45	1.10	1.02	2.00	2.00	2.00
$^{11}A_2$	0.43	1.08	2.00	2.00	2.00	1.03
$^{15}A_1$	0.43	1.09	1.02	2.00	2.00	2.00

[a] Energy difference between the corresponding electronic state and the $^{15}B_2$ state. [b] Electronic population of the Ni 4sp orbitals.

TABLE 7: Geometrical and Electronic Properties of $CoMo_2S_{10}H_6$ Cluster

electronic state	Co−Ss (Å)	SD(Ss)	Q_{Mo}	Q_{Ss}	Q_{Co}	4sp[a]
$^{16}A_1$	2.45	1.09	+0.11	−0.34	+1.39	0.45
$^{16}B_1$	2.45	1.08	+0.11	−0.34	+1.40	0.44
$^{16}B_2$	2.47	1.08	+0.11	−0.35	+1.42	0.44
$^{14}A_1$	2.43	0.96	−0.06	−0.37	+1.40	0.43
$^{14}A_2$	2.46	0.97	−0.07	−0.36	+1.42	0.43

electronic state	$3d_{xy}$	$3d_{xz}$	$3d_{yz}$	$3d_{x^2-y^2}$	$3d_{z^2}$	SD(Co)	ΔE[b] (kcal/mol)
$^{16}A_1$	1.10	1.02	1.02	1.99	1.99	2.88	0.00
$^{16}B_1$	1.10	2.00	1.02	1.67	1.34	2.89	+3.27
$^{16}B_2$	1.09	1.02	2.00	1.72	1.27	2.91	+6.85
$^{14}A_1$	1.10	1.02	2.00	1.70	1.32	2.86	+12.73
$^{14}A_2$	1.09	2.00	1.02	1.72	1.29	2.88	+15.07

[a] Electronic population of the Co 4sp orbitals. [b] Energy difference between the corresponding electronic state and the $^{16}A_1$ state.

the d^6 Ni configuration, they only report one electronic state and therefore it is not possible to compare their results with ours.

The $^{15}B_2$, $^{13}A_1$, and $^{15}A_1$ electronic states have the same electronic distribution for the Ni atom (See Tables 5 and 6), but different E_{ads} values (8.74, 6.12, and 5.55 kcal/mol respectively). These differences in the adsorption energies may be due to the HF scheme. Since, if the H_2S interaction is only with the Ni atom and this atom has the same electronic distribution in the $^{15}B_2$, $^{13}A_1$, and $^{15}A_1$ states, it is expected that the adsorption energies be equal.

Table 7 reports the geometry and electronic properties of the CoMo cluster obtained herein. The electronic properties of the $Mo_2S_{10}H_6$ moiety are equal for the first three electronic states ($^{16}A_1$, $^{16}B_1$, and $^{16}B_2$). The SD(Ss), Q_{Mo} and Q_S values are similar. These states are characterized mainly, by the 3d-electron distribution of the Co atom. For all states the Co has three unpaired electrons but different occupancies in the 3d orbitals

TABLE 8: Calculated Properties of H_2S Adsorption on $CoMo_2S_{10}H_6$ Cluster

Geometrical Properties

electronic state	Co−Ss (Å)	H_2S−Co (Å)	H−S (Å)	HSH (deg)	ΔE^a (kcal/mol)	E_{ads} (kcal/mol)
$^{16}A_1$	2.48	2.79	1.33	100.4	0.00	8.86
$^{16}B_1$	2.48	2.71	1.33	100.9	+2.04	10.09
$^{16}B_2$	2.50	2.64	1.33	101.3	+4.36	11.35
$^{14}A_1$	2.47	2.70	1.33	100.6	+13.17	8.42
$^{14}A_2$	2.48	2.76	1.33	100.4	+16.08	7.84

Electronic Properties

electronic state	Q_{Mo}	Q_{Ss}	Q_{Co}	Q_{H_2S}	SD(Ss)	SD(Co)
$^{16}A_1$	+0.12	−0.35	+1.40	+0.04	1.08	2.88
$^{16}B_1$	+0.12	−0.35	+1.40	+0.05	1.08	2.88
$^{16}B_2$	+0.13	−0.36	+1.41	+0.06	1.08	2.90
$^{14}A_1$	−0.04	−0.39	+1.39	+0.05	0.96	2.85
$^{14}A_2$	−0.05	−0.37	+1.42	+0.05	0.97	2.88

electronic state	4sp[b]	$3d_{xy}$	$3d_{xz}$	$3d_{yz}$	$3d_{x^2-y^2}$	$3d_{z^2}$
$^{16}A_1$	0.44	1.09	1.03	1.02	1.99	1.99
$^{16}B_1$	0.44	1.09	2.00	1.02	1.71	1.30
$^{16}B_2$	0.45	1.08	1.03	2.00	1.79	1.22
$^{14}A_1$	0.43	1.09	1.03	2.00	1.75	1.28
$^{14}A_2$	0.43	1.09	2.00	1.02	1.77	1.26

[a] Energy difference between the corresponding electronic state and the $^{16}A_1$state. [b] Electronic population of the Co 4sp orbitals.

and according to the orbital populations there is a mix between the $3d_{x^2-y^2}$ and $3d_{z^2}$ orbitals except for the $^{16}A_1$. This last state is 5.88 kcal/mol higher in energy than the $^{16}B_2$ state even though the Co atom has the same electronic distribution for both states. Therefore this energy difference can be attributed to the electronic state of the $Mo_2S_{10}H_6$ fragment.

Again, the magnitude of the charge transfer, the changes in the H_2S geometry, and the calculated adsorption energies (See Table 8) show that the H_2S molecule is physisorbed on the $CoMo_2S_{10}H_6$ cluster. The problem of the cancellation of the electronic effects of the $Mo_2S_{10}H_6$ fragment is clearly observed when comparing the $^{16}B_2$ with the $^{14}A_1$ state. For both states the electronic distribution on Co atom is the same but the adsorption energies differ in 3 kcal/mol. The fact that for different electronic states ($^{16}A_1$, $^{16}B_1$, and $^{16}B_2$) associated with different electron distribution on Co atom, the adsorption energies be quite close is a consequence of the physisorption phenomena. The physisorption does not change the electronic properties of the adsorption site and therefore could not stabilize or destabilize it. In all the cases studied here, there was a charge transfer from the metal to the $Mo_2S_{10}H_6$ fragment. This result is in agreement with previous theoretical results that explain the catalytic in terms of an electron transfer from the metal to the Mo[8,36−37]

Vertical Adsorption. Mode B. Figure 2b displays the geometrical arrangement and Table 9 shows ab initio SCF results for the second adsorption mode of H_2S on $XMo_2S_{10}H_6$ clusters (X = Co, Ni, Cu, Zn). Figure 3 display the potential energy curves for each one of the electronic states shown in Table 9. All potential curves exhibit a minimum of energy, which is an indication of attractive interactions. The horizontal solid line corresponds to zero adsorption energy. Therefore, the potential curves above this line represent adsorptions that are not energetically favored. Only three curves have a minimum below this line and correspond to the Co, Ni, and Zn cases. For Cu the curve is above the zero line showing that a metastable molecular aggregate exists but it is not energetically favored.

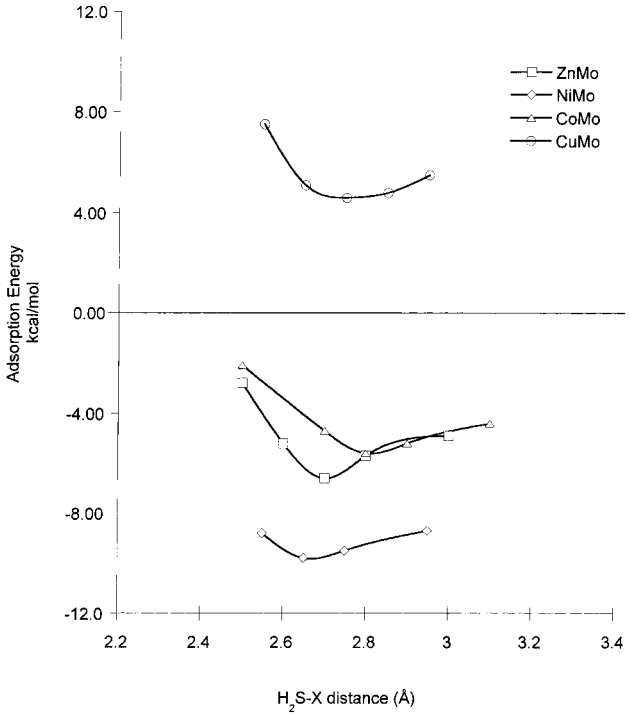

Figure 3. Potential energy curves for sorption, Mode B, of H_2S molecule on different $XMo_2S_{10}H_6$ (X = Co, Ni, Cu, Zn) clusters.

TABLE 9: Calculated Properties of H_2S Adsorption (Mode B) on $XMo_2S_{10}H_6$ Cluster X = Co, Ni, Cu, Zn

Geometrical Properties

electronic state (X atom)	X-Ss (Å)	H_2S−X (Å)	H−S (Å)	HSH (deg)	[a]E_{ads} (kcal/mol)
$^{16}A_2$ (Co)	2.51	2.78	1.33	100.7	+5.6
$^{15}B_2$ (Ni)	2.45	2.66	1.33	100.9	+9.8
$^{12}B_1$ (Cu)	2.57	2.73	1.33	100.1	−4.6
$^{11}B_2$ (Zn)	2.45	2.68	1.33	100.8	+6.1

Electronic Properties

electronic state (X atom)	SD(Ss)	Q_{Mo}	Q_{Ss}	Q_X	Q_{H_2S}	SD(X)
$^{16}A_2$ (Co)	1.09	+0.08	−0.35	1.46	+0.04	2.97
$^{15}B_2$ (Ni)	0.90	+0.03	−0.48	1.43	+0.10	1.90
$^{12}B_1$ (Cu)	1.30	+0.04	−0.12	+0.75	+0.04	0.04
$^{11}B_2$ (Zn)	1.06	−0.10	−0.32	+1.44	+0.05	0.03

[a] Adsorption energy.

This type of metastable structure has been previously reported in the literature for the case of carbon adsorption on Ni clusters.[38] The authors showed that a geometry optimization of the cluster (relaxation) favors the adsorption but more important than the cluster relaxation is the coordination of the atoms that forms the adsorption site. Therefore, if relaxation process is carry out on $XMo_2S_{10}H_6$ fragment it is possible that the adsorption energy be improved but it cannot change the order: $E_{ads}(Cu) < E_{ads}(Co) < E_{ads}(Zn) < E_{ads}(Ni)$ because the coordination of the adsorption site remains unchanged. In general, the surface relaxation and reconstruction are consequences of chemisorption and not of physisorption processes[39,40]

Numerical values for the geometrical and electronic properties at minima of the potential energy curves are listed in Table 9. The results for Co, Ni, and Zn show again that the interaction phenomenon corresponds to a physisorption, which leaves the geometrical and electronic structure of the H_2S molecule almost unperturbed.[40] The geometrical and electronic properties are similar to those found for the adsorption mode A (see Tables 8 and 6). Again, the results for the Ni system are similar to the reported in the ref 10. A particularly striking case is the $^{12}B_1$ state of the $H_2S-CuMo_2S_{10}H_6$ aggregate. In the adsorption mode A, the Cu atom has one unpaired electron and a high positive charge (SD(Cu) = 0.90, $Q_{Cu} = +1.39$). In the mode B we found for the corresponding state, that the Cu atom has a closed-shell structure and a low positive net charge ($Q_{Cu} = +0.75$). In this low oxidation state the Cu atom is not capable to stabilize the interaction H_2S-Cu and therefore it produces a weakly bonded state (See Figure 3).

In general, the H_2S adsorption process on metal sulfide or promoted metal sulfide is not simple. The exact nature of the adsorption sites is not known. Various mechanisms have been proposed to explain the experimental results.[18−20,41−43] Examining the effects of several metal promoters on the sulfidation of Mo, Rodriguez et al.[8,44−46] found that the net effect of the promoters is to increase the reactivity of Mo toward sulfur. The trend found for the sulfidation of Mo compares well with the trend observed in the HDS activity, i.e., Co and Ni atoms significantly enhance the Mo−S interactions whereas the effect of Cu and Zn is weak. These and our results suggest that the adsorption of H_2S could occur preferentially on activated Mo and not on the metal promoter. As previously suggested by Kabe et al.,[17] the promotion effect may be due to the addition of the second metal which decreases the strength of sulfur−molybdenum bond. Therefore, the formation, adsorption, or desorption of H_2S becomes easier on promoted MoS_2 than on unpromoted MoS_2 catalysts. On the other hand, recent experimental results have shown that the promotional effect could be to provide H atoms for the hydrogenation[47] or to transport the reactants to the active site on the catalytic surface.[48]

It is well know from the literature that the interaction of the H_2 with the HDS catalysts is complex. Theoretical and isotopic exchange studies show that the cleavage of H−H and H−S bonds occurs during the catalytic process and that the homolytic as well as the heterolytic cleavages of the H_2 molecule are possible. On the other hand, the hydrogen is sorbed on the MoS_2 and the real composition of the catalyst seems to be H_xMoS_2. This sorbed hydrogen favors the reaction of isomerization and hydrogenation of olefins but inhibit, for example, the isotopic exchange H_2-D_2.[49]

Zakharov, Startsev, et al.[11,12] have studied, from the theoretical point of view, the effect of the H sorbed on the CoMoS and NiMoS catalyst. They show that the adsorption energy of H_2S on the NiMoS catalysts changes from 82.8 kJ/mol[10] to 267.1 kJ/mol[11] when an occluded hydrogen atom (H_o) is included in the modeling. This result points out that the H_2S adsorption is highly favored in the presence of the occluded H_o. For (H_o)CoMoS, Zakharov and Startsev report[12] an adsorption energy of 16.6 kcal/mol at Hartree−Fock level, a value that is higher than the values found by us (see Table 8) with the model of catalyst that does not include the H_o. This corroborates the importance of the sorbed hydrogen. Besides this, in the (H_o)CoMoS and (H_o)NiMoS models both metals, the Co as well the Ni, have a d^6 configuration while in our models the Co has a d^7 configuration and the Ni has a d^8 configuration. This last result seems to indicate that the oxidation state of the metal strongly affects the H_2S adsorption energy.[12,50]

Conclusions

A summary of the most relevant features found in this work is as follow. (a) The calculated adsorption energy does not correlate with the experimental catalytic activity (CA(Mo−Ni) > CA(Mo−Co) > CA(Mo−Cu) > CA(Mo−Zn)). (b) The distance H−S, in the H_2S molecule, does not change after the adsorption and only small changes in the angle H−S−H were observed. (c) In all cases, a small charge transfer (around 0.05e) from the H_2S molecule to the $XMo_2S_{10}H_6$ clusters occurs. (d) This charge is received by the $Mo_2S_{10}H_6$ moiety, showing that the $Mo_2S_{10}H_6$ structure contributes to the stabilization of the $H_2S-XMo_2S_{10}H_6$ system receiving the transferred charge from the adsorbed molecule. (e) The positive charge on X atom comes from the partial charge transfer of the 4s electrons to the $Mo_2S_{10}H_6$ fragment.

It is well-known that the physisorption leaves the electronic and geometric structures of the adsorbate unperturbed whereas in the chemisorption, the electronic and geometric structures of the adsorbate change substantially.[40] Therefore, from the analysis of the relevant features we can conclude that the vertical sorption of H_2S on $XMo_2S_{10}H_6$ clusters corresponds to a physisorption instead of a chemisorption. The vertical sorption of H_2S on $XMo_2S_{10}H_6$ does not modify the electronic properties of the X atom nor does it stabilize the active site of the bimetallic species and cannot be considered an important step in the HDS reaction. Other adsorption modes and models are currently under study.

On the other hand, this work shows the importance of searching among different multiplicities in order to analyze the electronic properties of the $XMo_2S_{10}H_6$ systems. Even if the calculations are done at Post-HF level, it is necessary to investigate all possible states.

Acknowledgment. The authors acknowledge the financial support given by CONICIT (Grant S1-96001399).

References and Notes

(1) Startsev, A. N. *Catal. Rev. Sci. Eng*. **1995**, *37*, 353.
(2) Chianelli, R. R.; Daage, M.; Ledoux, M. J. *Adv. Catal*. **1994**, *40*, 177.
(3) Chianelli, R. R.; Pecorano, T. A.; Halbert, T. R.; Pan, W. H.; Stiefel, E. I. *J. Catal*. **1984**, *86*, 226.
(4) Harris, S.; Chianelli,to R. R. *J. Catal*. **1986**, *98*, 17.
(5) Prins, R.; De Beer, V. H.; Somerjai, J. G. A. *Catal. Rev. Sci. Eng*. **1989**, *31*, 1.
(6) Vasudevan, P. T.; Fierro, J. L. *Catal. Rev. Sci. Eng*. **1996**, *32*, 161.
(7) Topsoe, H.; Clausen, B. S. *Catal. Rev. Sci. Eng*. **1984**, *26*, 395.
(8) Rodriguez, J. A. *J. Phys. Chem. B* **1997**, *101*, 7524.
(9) Harris, S. *Polyhedron* **1986**, *5*, 151.
(10) Zakharov, I. I.; Startsev, A. N.; Zhidomirov, G. M. *J. Mol. Catal*. **1997**, *119*, 437.
(11) Zakharov, I. I.; Startsev, A. N.; Zhidomirov, G. M.; Parmon V. N. *J. Mol. Catal. A: Chemical* **1999**, *137*, 101.
(12) Zakharov, I. I.; Startsev, A. N *J. Phys. Chem. B* **2000**, *104*, 9025.
(13) Toulhoat, H.; Raybaud, P.; Kasztelan, S.; Kresse, G.; Hafner, J. *Catal. Today* **1999**, *50*, 629.
(14) Norskov, J. K.; Clausen, B. S.; Topsoe, H. *Catal. Lett.* **1992**, *13*, 1.
(15) Leglise, J.; van Gestel, J. N. M.; Finot, L.; Duchet, J. C.; Dubois, J. L. *Catal. Today* **1998**, *41*, 347.
(16) Locrenay, E.; Sakanish, K.; Mochida, I. *Catal. Today* **1997**, *39*, 13.
(17) Kabe, T.; Qian, W.; Ishihara, A. *Catal. Today* **1997**, *39*, 3.
(18) d'Ararujo, P.; Thomas, C.; Vivier, L.; Duprez, D.; Pérot, G. *Catal. Lett*. **1995**, *34*, 375.
(19) Massoth, F. E.; Zeuthen, P. *J. Catal*. **1994**, 145, 216.
(20) Thomas, C.; Viver, L.; Lemberton, J. L.; Kasztelan, S.; Pérot, G. *J. Catal*. **1997**, *167*, 1.

(21) Kabe, T.; Qian, W.; Wang W.; Ishihara, A. *Catal. Today* **1996**, *29*, 197.
(22) Startsev, A. N. *J. Mol. Catal. A: Chemical* **2000**, *152*, 1.
(23) Frisch, M. J.; Trucks, G. W.; Schlegel, H. B.; Gill, P. M. W.; Johnson, B. G.; Robb, M. A.; Cheeseman, J. R.; Keith, T.; Petersson, G. A.; Montgomery, J. A.; Raghavachari, K.; Al-Laham, M. A.; Zakrzewski, V. G.; Ortiz, J. V.; Foresman, J. B.; Cioslowski, J.; Stefanov, B. B.; Nanayakkara, A.; Challacombe, M.; Peny, C. Y.; Ayala, P. Y.; Chen, W.; Wong, M. W.; Andres, J. L.; Replogle, E. S.; Gomperts, R.; Martin, R. L.; Fox, D. J.; Binkey, J. S.; Defrees, D. J.; Baker, J.; Stewart, P. J.; Head-Gordon, M.; Gonzales, C.; Pople, J. A. *Gaussian 94*, Revision D.4; Gaussian, Inc.: Pittsburgh, PA, 1995.
(24) Stevens, W.; Basch, H.; Krauss, M. J. *Chem. Phys.* **1984**, *81*, 6026.
(25) NBO Version 3.1; Glendening, E. D.; Reed, A. E.; Carpenter, J. E.; Weinhold, F.
(26) Reed, A. E.; Curtiss, L. A.; Weinhold, F. *Chem. Rev.* **1988**, *88*, 899.
(27) Anderson, A. B.; Hong, S. Y.; Smialek, J. L. *J. Phys. Chem.* **1987**, *91*, 4250.
(28) Pis Diez, R.; Jubert, A. H. *J. Mol. Catal.* **1992**, *73*, 65.
(29) Serfaco, S. J.; Passeggi, M. C. G. *J. Phys. Chem.* **1985**, *18*, 3717.
(30) NieMann, W.; Clausen, B.; Topsoe, H. *Catal. Lett.* **1990**, *4*, 355.
(31) Bouwens, S. M. A. M.; Koningsberger, D. C.; De Beer, V. H. J.; Louwers, S. P. A.; Prins, R. *Catal. Lett.* **1990**, *5*, 273.
(32) Wyckoff, R. W. G. *Crystal Structure*; Krieger: New York, 1963; p 280.
(33) Smit, T. S.; Johnson, K. H. *J. Mol. Catal.* **1994**, *91*, 207.
(34) Sierraalta, A.; Ruette, F. *J. Mol. Catal.* **1996**, *109*, 227.
(35) Whiyyen, J. L.; Yang, H. *Surf. Sci. Rep.* **1996**, *24*, 55.
(36) Zonnevylle, M.; Hoffman, R.; Harris, S. *Surf. Sci.* **1990**, *199*, 320.
(37) Smit, T. S.; Johnson, K. H. *Catal. Lett.* **1994**, *28*, 361.
(38) Poveda, F. M.; Sierraalta, A.; Villaveces, J. L.; Ruette, F. *J. Mol. Catal.* **1996**, *106*, 109.
(39) van Santen, R. A.; Neurock, M. *Catal. Rev. Sci. Eng.* **1995**, *37*, 557.
(40) Hermann, K.; Witko, M. *J. Mol. Struct. (THEOCHEM)* **1999**, *458*, 81.
(41) Yang, S. H.; Satterfield, C. N. *J. Catal.* **1983**, *81*, 168.
(42) Olade, A.; Pérot, G. *Appl. Catal.* **1985**, *13*, 373.
(43) Thomas, C.; Viver, L.; Travert, A.; Maugé, F.; Kasztelan, S.; Pérot, G. *J. Catal.* **1998**, *179*, 495.
(44) Rodriguez, J. A. *Polyhedron* **1997**, *16*, 3177.
(45) Li, S. Y.; Rodriguez, J. A.; Hrbek, J.; Huang, H. H.; Xu, G. Q. *Surf. Sci.* **1996**, *266*, 29.
(46) Kuhn, M.; Rodriguez, J. A. *Surf. Sci.* **1996**, *355*, 85.
(47) Rodriguez, J. A.; Dvorak, J.; Capitano, A. T.; Gabelnick, A. M.; Gland, J. L. *Surf. Sci.* **1999**, *429*, L462.
(48) Kushmerick, J. G.; Kandel, S. A.; Han, P.; Johnson, J. A.; Weiss, P. S. *J. Phys. Chem. B* **2000**, *104*, 2980.
(49) Komatsu, T.; Hall, W. K. *J. Phys. Chem.* **1992**, *96*, 8131.
(50) Rodriguez, J. A.; Dvorak, J.; Jirsak, T. *J. Phys. Chem. B* **2000**, *104*, 11515.